

Automatic Snake Gait Generation Using Model Predictive Control

Emily Hannigan, Bing Song, Gagan Khandate, Maximilian Haas Heger, Ji Yin and Matei Ciocarlie

Abstract—In this paper, we propose a method for generating undulatory gaits for snake robots. Instead of starting from a pre-defined movement pattern such as a serpenoid curve, we use a Model Predictive Control approach to automatically generate effective locomotion gaits via trajectory optimization. An important advantage of this approach is that the resulting gaits are automatically adapted to the environment that is being modeled as part of the snake dynamics. To illustrate this, we use a novel model for anisotropic dry friction, along with existing models for viscous friction and fluid dynamic effects such as drag and added mass. For each of these models, gaits generated without any change in the method or its parameters are as efficient as Pareto-optimal serpenoid gaits tuned individually for each environment. Furthermore, the proposed method can also produce more complex or irregular gaits, e.g. for obstacle avoidance or executing sharp turns.

I. INTRODUCTION

Snake robots have great potential in challenging environments due to their many degrees of freedom (DoF), providing them with the ability to adapt to cluttered and complex terrain [1], [2], [3]. However, the large number of DoF also makes generating efficient locomotion gaits a significant challenge. As a result, significant work has focused on snake robot gait synthesis, starting with the mathematical approximation of their biological counterparts.

The serpenoid curve [1] and the serpentine curve [4] approximate snake lateral undulation for locomotion over flat surfaces. More recently, central pattern generators inspired by neural activity have been used to produce rhythmic patterns as snake gaits[5]. Realization of these gaits on a robot mechanism is usually done through position control of the robot’s joint angles [1], [6], [2], [7]. Based on predefined gait patterns like the serpenoid curve, perception-driven obstacle-aided snake robots are able to perform complex gaits against their terrain like the biological snakes [8].

However, different environments are characterized by what we refer to as different *reaction forces*: these can include dry friction (for land snakes), viscous friction (for undulatory movement in water at a regime with a low Reynolds number), or fluid dynamic effects like added mass (for movement in water at a regime with a high Reynolds number). Predefined movement patterns (such as a serpenoid curve) generally require hand-tuning in order to achieve efficient gaits in each of these environments [9], [10]. Finding the serpenoid gait parameters that achieve a specific velocity, or that minimize power consumption for a given velocity, is a manual process, and the resulting parameters rarely transfer to different

All authors are with the Dept. of Mechanical Engineering, Columbia University, NY. E-mail: {ejh2192, bs2664, gk2496, mkh2149, jy2917, mtc2103}@columbia.edu

environmental conditions. Even compliant controllers that exhibit remarkable adaptability to obstacles [7] are still designed or hand-tuned specifically for an underlying model of surface friction. Synthesising efficient gaits across different environmental conditions, without changing the locomotion algorithm or its parameters, remains a challenging problem.

In this paper, we propose an optimal control approach to gait generation that does not start from a pre-defined movement pattern. Instead, based on a model of snake dynamics, the algorithm attempts to produce trajectories that minimize a given cost function. By choosing an appropriate cost function (e.g. distance to a goal), we show that this approach produces effective locomotion gaits. Importantly, this approach produces efficient gaits across multiple different environments: as long as the appropriate environment reaction forces are modeled as part of the dynamics, the algorithm automatically produces an efficient gait adapted to the environment type. The resulting gaits are comparable to the baseline of the Pareto-optimal serpenoid gaits. Furthermore, our approach readily transfers between different environments, with no tuning or change in parameters.

While matching the performance of a pre-defined serpenoid gait for straight-line locomotion, the optimal control approach can also synthesise more complex gaits, depending on the requirements of the task. For example, we show that this approach can generate gaits for passing through narrow tunnels, or for taking sharp turns. In each case, the only modification needed is in the cost function, which must reflect the requirements of each task, such as maintaining distance from the obstacles or reaching a desired point.

Overall, the main contributions of our paper include:

- We show that optimal control methods can generate effective undulatory gaits for snake robots without starting from a predefined movement pattern. When this approach is applied using different models for environment reaction forces, it produces different gaits, each suited to its environment, without any change of the algorithm or tuning of its parameters. These gaits show both locomotion and energy efficiency.
- We introduce a novel model of anisotropic Coulomb friction, and use it to model land snakes that exhibit side slip. Together with existing models for anisotropic viscous friction, drag force and added mass effects in fluids, we can model a wide range of environments for snake locomotion.
- We also show that snake gaits obtained via optimal control exhibit additional desirable properties, such as the ability to perform sharp turns, as well as pass through narrow obstacles without making contact.

II. RELATED WORK

Previous work on snake gait generation generally focuses on producing compliant motion across unstructured surface terrains or in fluids. To achieve such compliant motion, [11] used low level torque controllers. After this [7] developed the shape-compliant control method that adapts snake gaits through an irregularly spaced peg array. [2] applied integral line-of-sight guidance control for underwater snake robots to adapt to ocean currents of unknown direction and magnitude. Other nonlinear algorithms like sliding mode control [12] and mixed integer programming [13] have also been investigated to produce gaits.

On top of being able to adapt to unstructured terrain, gaits also need to be efficient to be practical in real world applications. Gait efficiency has been improved by [14], [15], [16]. Recently, [17] developed a decentralized control method that improved the locomotion efficiency of a the compliant controller [7] by 40%.

In this paper we use an optimal control method, i.e., MPC, to automatically generate effective gaits across multiple environments without human intuition or retuning of parameters. The MPC algorithm we use is iterative linear-quadratic-regulator (iLQR), a very successful example of locally-optimal control for nonlinear dynamical systems that has been applied on legged robots [18].

Existing work on modeling undulatory locomotion either assumes a sideslip constraint [19], or anisotropic friction applied to the robot links [20]. In this paper we model the locomotion with the assumption of anisotropic friction. Using the maximum dissipation principle [21], we have derived a more accurate anisotropic Coulomb friction model and apply this to simulate surface friction. For underwater robots, dynamics has been studied in the fluids of different Reynolds numbers [22], [2], [23], [24]. At low Reynolds numbers, viscous friction is the dominating reaction force. At high Reynolds numbers, added mass and drag (fluid dynamics) dominates. We also include these dynamic models to simulate different environments.

A common method to evaluate gait efficiency is the Pareto curve which shows the trade-off between locomotion speed and energy consumption [20], [15], [16]. We use this method to create a baseline to evaluate out auto-generated gaits.

III. DYNAMIC MODEL

The dynamics of snake locomotion are well studied in the literature, as a dynamic model is often used to validate or tune a proposed gait. In our work, the dynamic model is also used to generate the trajectory, via optimization with respect to a given cost function. Before describing the gait synthesis method, we will thus describe the dynamic model we use, which follows a standard time-stepping method based on a Newton-Euler formulation with explicit integration for a 2D n-link kinematic chain.

We employ the model depicted in Fig. 1, where q_i denotes the relative angle of link i with respect to the previous link (counterclockwise); τ_i is the motor torque applied to joint i ; and $\mathbf{p}_0 = [x_0, y_0]$ is the head position in the global

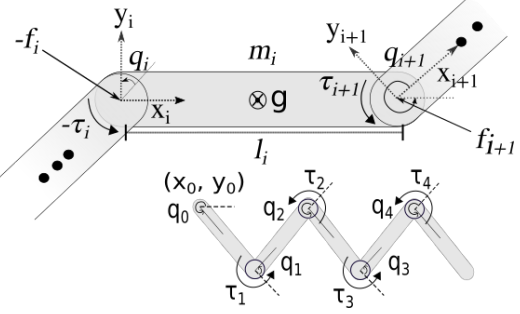


Fig. 1. Illustration of the structure and dynamic model of the snake robot. The top figure shows link i , its axes, torques, mass, and length. The bottom figure shows an example of a 5-link snake.

coordinates. The length of link i is l_i and its weight is denoted by m_i . We assume uniform distribution of mass so the center of gravity is located in the middle of each link. Each link has a local coordinate frame based at the proximal end, with the y_i axis pointing in the longitudinal direction and the x_i axis in the transverse direction.

According to Newtonian dynamics, at any time step, force equilibrium on link i expressed in the local coordinate frame requires:

$$-\mathbf{f}_i + R_i^{i+1} \mathbf{f}_{i+1} = m_i \mathbf{a}_{ci} - m_i g R_w^i \begin{bmatrix} 0 \\ -1 \end{bmatrix} + \mathbf{f}_i^{env} \quad (1)$$

$$\mathbf{a}_{ci} = \mathbf{a}_i + 0.5l_i \dot{\omega}^i \begin{bmatrix} 0 \\ 1 \end{bmatrix} + 0.5l_i \omega_i^2 \begin{bmatrix} -1 \\ 0 \end{bmatrix} \quad (2)$$

where \mathbf{f}_i is the internal force applied by link $i+1$ to link i in the local coordinates; R_i^{i+1} is the rotation matrix from the local coordinates $i+1$ to the local coordinates i ; \mathbf{a}_{ci} is the acceleration of the center of mass of link i . Of particular interest is the vector \mathbf{f}_i^{env} , which denotes external forces applied by the environment in response to the snake movement. We dub these "reaction forces", and discuss them in detail in the following section.

Similarly, torque equilibrium on link i requires:

$$-\tau_i + 0.5l_i [0 \ 1] (\mathbf{f}_i + R_i^{i+1} \mathbf{f}_{i+1}) + \tau_{i+1} = \dot{q}_i \mu_v \quad (3)$$

where τ_i is the torque applied by link $i+1$ to link i ; μ_v is the joint viscous friction coefficient. Additional constraints follow from the consistency of angular and linear accelerations between consecutive links, with no grounding on the first joint:

$$\dot{\omega}_{i-1} + \ddot{q}_i - \dot{\omega}_i = 0 \quad (4)$$

$$R_i^{i+1} (\mathbf{a}_{i-1} + l_{i-1} \dot{\omega}_{i-1} \begin{bmatrix} 0 \\ 1 \end{bmatrix} + l_{i-1} \omega_{i-1}^2 \begin{bmatrix} -1 \\ 0 \end{bmatrix}) = \mathbf{a}_i \quad (5)$$

$$\mathbf{f}_0 = 0 \quad (6)$$

For known motor torques τ_i , we can now solve the system (1)-(6) for unknowns \mathbf{f}_i , $\dot{\omega}_i$, \mathbf{a}_i , \dot{q}_i . We then use numerical integration to advance to the next time step, by computing q_i , \dot{q}_i from \dot{q}_i and \mathbf{p}_0 from \mathbf{a}_0 . We note that multiple numerical integration methods can be used for this procedure. In our work, we use the more accurate RK4 integration method when using this model for validation, and the faster

Euler method when using the model for gait synthesis, as we will describe in the next sections.

IV. MODELING ENVIRONMENTS

Biological snakes can achieve undulatory motion in many types of environments (e.g. overland, underwater) and at many scales. In each case, they achieve this by creating or leveraging anisotropic effects in the reaction forces applied by the environment in response to their motion. However, the exact nature of these forces varies greatly between environments, giving rise to different strategies: during locomotion, some snakes adjust their scales, other redistribute their weight or change their winding angles, etc. [25]). These strategies produce different gaits, each suited to its environment.

We can attempt to capture the characteristics of a given environment by using an appropriate model for the reaction forces applied in our dynamics formulation described previously. We use the broader term "reaction forces" to encompass both frictional and non-frictional effects which contribute to locomotion. In this work, we use three such models, described below.

A. Dry friction

The most commonly used model for simulating dry frictional contact is that of Coulomb friction [26], [21]. For undulatory motion over solid, dry surfaces (e.g. overland snakes not moving on granular media), anisotropic effects can be captured by using different friction coefficients for longitudinal vs. transverse friction forces. However, the Coulomb friction model introduces non-linear and non-convex constraints that are difficult to solve efficiently. A simplified version, similar to the model used in previous studies on snake robot locomotion [9], [27], [1] is:

$$\mathbf{f}_{\text{box}}^{\text{env}} = -mg \begin{bmatrix} \mu_l & 0 \\ 0 & \mu_t \end{bmatrix} \text{sgn}(\begin{bmatrix} v_l \\ v_t \end{bmatrix}) \quad (7)$$

where μ_t is the transverse friction coefficient and μ_l is the longitudinal coefficient.

However, this simplified model has multiple limitations. First, applied friction direction as a function of contact velocity (relative velocity of the link w.r.t the ground) is non-smooth. Second, it does not obey the Maximum Dissipation Principle [21], which states that, given a contact velocity v , the ensuing friction force \mathbf{f} maximizes energy dissipation (i.e., $-\mathbf{f}v$), subject to other constraints (such as friction coefficients). We thus introduce a new model for anisotropic dry friction, formulated as:

$$\mathbf{f}_{\text{dry}}^{\text{env}} = \begin{bmatrix} \mu_l & 0 \\ 0 & \mu_t \end{bmatrix} \begin{bmatrix} \sin(\arctan(\frac{\mu_t v_t}{\mu_l v_l})) \\ \cos(\arctan(\frac{\mu_t v_t}{\mu_l v_l})) \end{bmatrix} \quad (8)$$

where v_t is the transversal component of the velocity of the center of mass, and v_l is the longitudinal component.

This new dry friction model Eq. (8) is derived by maximizing the dissipation $-\mathbf{f}v$ with the assumption that the anisotropic friction is represented by a friction ellipse with the major axis equal to μ_t and the minor axis equal to μ_l as shown in Fig. 2.

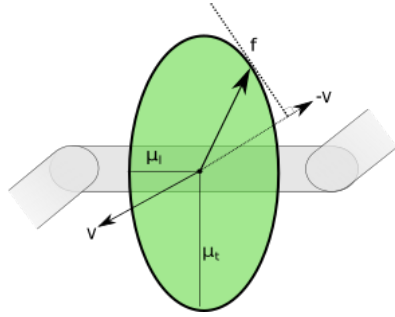


Fig. 2. Proposed dry friction model. Selected friction direction maximizes energy dissipation under anisotropic friction constraints.

B. Viscous friction

For underwater undulatory locomotion, anisotropic viscous friction plays an important role for generating forward motion. At low Reynolds number (i.e. small scale organisms in water), it can be considered the dominant reaction force. A model of reaction forces that comprises viscous friction exclusively can be considered as an approximation for small scale swimmers, such as tadpoles. We note that viscous friction has occasionally been used in the literature to model overland snakes as well [2], even though it is a less accurate approximation of dry Coulomb friction than the box model discussed above. We model viscous friction as:

$$\mathbf{f}_{\text{viscous}}^{\text{env}} = \begin{bmatrix} c_l & 0 \\ 0 & c_t \end{bmatrix} \begin{bmatrix} v_l \\ v_t \end{bmatrix} \quad (9)$$

where c_l and c_t are the longitudinal viscous friction coefficient and the transversal friction coefficient respectively.

C. Added mass

In fluids of high Reynolds number, drag and added mass effect are the dominating reaction force. Added mass is particularly important for modeling large undewater snakes or eels because their bodies displace a significant volume of water during locomotion.

We assume the links are cylindrical with a cross section of height a and width b . The length of the link is denoted by l [23] [24]. We compute the drag force as:

$$\mathbf{f}_{\text{fluids}}^{\text{env}} = \begin{bmatrix} -\frac{1}{2}pC_d a l & 0 \\ 0 & -\frac{1}{2}p\pi C_f \frac{a+b}{4} l \end{bmatrix} \begin{bmatrix} \text{sgn}(v_l)v_l^2 \\ \text{sgn}(v_t)v_t^2 \end{bmatrix} \quad (10)$$

where p is fluid density, and C_f and C_d are the drag coefficients in the longitudinal and transverse directions.

In addition, the volume of fluid displaced during motion has the effect equivalent to adding mass to the links of the snake. However, due to the shape of the link, this effect is anisotropic, with more mass added for motion in the transverse direction. In Eq. (1), we must thus distinguish between added mass in the transverse vs. longitudinal directions:

$$-\mathbf{f}_i + R_i^{i+1} \mathbf{f}_{i+1} = \mathbf{M}_i \mathbf{a}_{ci} - g \mathbf{M}_i R_w^i \begin{bmatrix} 0 \\ -1 \end{bmatrix} + \mathbf{f}_i^{\text{env}} \quad (11)$$

where we compute the added mass using:

$$\mathbf{M}_i = \begin{bmatrix} m_i & 0 \\ 0 & m_i + m_i^{add} \end{bmatrix} \quad (12)$$

$$m_i^{add} = p\pi C_a \frac{a^2}{4} l \quad (13)$$

V. GAIT SYNTHESIS METHOD

For gait synthesis, we use a Model Predictive Control (MPC) method, which relies on an internal model of the dynamics of the system in order to repeatedly optimize a control sequence. MPC provides a well-established toolset of optimization method, a review of which is beyond the scope of this paper; we provide here a short overview, then focus on applicability to snake locomotion. Given a (potentially nonlinear) dynamic model

$$\mathbf{x}(t+1) = f(\mathbf{x}(t), \mathbf{u}(t)) \quad (14)$$

where \mathbf{x} denotes the state and \mathbf{u} denotes the control action, MPC computes the optimal action sequence $\mathbf{u}(i)$ ($i = t, t+1, \dots, t+N-1$) that minimizes a cost function

$$J = \sum_{i=t}^{t+N-1} l(\mathbf{x}(i), \mathbf{u}(i)) + l_f(\mathbf{x}(t+N)) \quad (15)$$

where N is the horizon length; $l(\mathbf{x}(i), \mathbf{u}(i))$ is the cost of the state and action at time i , and $l_f(\mathbf{x}(t+N))$ is the cost on the final state of this horizon. The specific optimization algorithm we use is iLQG [18], a variant of the iterative Linear Quadratic Regulator previously demonstrated on problems such as legged locomotion and manipulation.

After an optimized trajectory has been computed, the robot takes the first (or the first few) action(s) therein, and the process restarts from the new robot state. This allows the robot to compensate for errors which inevitably arise when following a given trajectory, due to the linearization of the dynamics model, or simply due to errors in the model.

A. Application to Gait Synthesis

For an n -link snake robot, we define the state vector as $\mathbf{x} = [x_0 \ y_0 \ q_0 \ \dots \ q_l \ \dot{x}_0 \ \dot{y}_0 \ \dot{q}_0 \ \dots \ \dot{q}_n]^T$, and the action vector $\mathbf{u} = [\tau_1 \ \dots \ \tau_n]$. The dynamic model $f(\mathbf{x}(t), \mathbf{u}(t))$ is computed as described in Sec. III. We use finite differencing to compute the derivatives of this model w.r.t. the state and action vectors, both of which are needed by the optimization routine.

For generating locomotion gaits without obstacles, we use the following cost functions:

$$l(\mathbf{x}, \mathbf{u}) = \alpha \|\mathbf{p}_{goal} - \mathbf{p}_0\| + \beta \sum_{j=1}^n \tau_j^2 \quad (16)$$

$$l_f(\mathbf{x}) = \alpha \|\mathbf{p}_{goal} - \mathbf{p}_0\| \quad (17)$$

where \mathbf{p}_{goal} is the desired position of the head of the snake and α and β are tunable parameters.

For obstacle avoidance, we use an additional term that takes into account the relative position of each segment of the snake robot with respect to each obstacle. In other words, all of the obstacles in the environment and all of the segments of

TABLE I
PARAMETERS OF THE SNAKE ROBOT AND REACTION FORCES

l_i [m]	a [m]	b [kg]	m_i	μ_t	μ_l	c_t	c_l	C_f	C_d	C_a	p [kg·m ³]
.2	.15	.05	.2	.9	.1	1	10	.01	1	1	1000

the snake contribute to this term. The distance between each obstacle and each snake segment is calculated as d_{ij} , where i is the index for obstacles, and j is the index for segments. We note that negative distance indicates that a snake segment is interpenetrating with an obstacle. The obstacle cost is the sum of 2-dimensional Heaviside step functions for every d_{ij} :

$$l^{obs}(\mathbf{x}, \mathbf{u}) = \sum_{i=1}^k \sum_{j=1}^n \frac{A}{1 + e^{2kd_{ij}}} \quad (18)$$

where k denotes the number of obstacles, and A is a parameter that determines the rise of the step function. In all of our experiments we set $A = 1$.

VI. RESULTS

We test the proposed gait generation method using a five link snake robot in different environments, each based on one of the reaction forces models described in Sec. IV. The parameters of the snake robot and reaction forces are summarized in Table I. Torques at the joints are capped at 1 N · m. All gaits are tested in simulation using the model described in Sec. III with RK4 integration.

A. Baseline: Serpenoid Curve Gaits

As a comparison baseline for the generated gaits, we will compare performance to that obtained by using pre-defined serpenoid curves. For each joint i , desired joint angle as a function of time is defined as:

$$q_i(t) = \alpha \sin(2\pi ft + (i-1)\beta) + \gamma \quad (19)$$

where f , α , and β are the parameters that can be used to tune the behavior of the resulting gait. In practice, this desired trajectory at each joint can be tracked using PID control, resulting in locomoting gaits.

As described earlier, one of the key difficulties for using serpenoid curves is the need to tune the curve parameters in order to obtain the desired behavior. To find the most effective gaits, we carried out a grid search over curve parameters; the boundaries and step size of the grid search are listed in Table II. Furthermore, we found the performance of the resulting gaits to also be highly sensitive to the gains of the controller used to track the serpenoid curve; we thus included these gaits in our grid search.

We evaluated all gaits in our grid search in terms of speed and power consumption. For each combination of parameters, we generated a 6 s trajectory, with the snake starting from the rest. To minimize the effect of the chosen start pose on gait performance, we considered the first 2 s of the trajectory to be "ramp up" time, and only measured speed and power over the last 4 s. Figure. 3 plots the power consumption versus the forward speed of each serpenoid curve (blue circles). The black line is the Pareto-optimal front [28] that represents the best tradeoff between power

TABLE II

SERPENOID CURVE AND PD CONTROLLER GRID SEARCH PARAMETERS

Gait Param	Grid Search Space		
	Min	Max	Interval
f	0.5	10.0	0.25
α	0.1π	1.0π	0.1π
β	0.5π	4.0π	0.1π

Gain	Grid Search Space		
	Min	Max	Interval
P	0.1	3.0	0.1
D	0.05	0.2	0.01

consumption and locomotion speed. Gaits on this Pareto curve need produce theis corresponding forward speeds with the lowest power consumption.

B. Synthesized Gaits and Environment Generalizability

We used the proposed MPC-based methods to synthesize gaits accross all the environments described so far. We tested 9 sets of parameters of the quadratic cost, i.e., $\alpha = 1$, $\beta = 0.1$, 0.01 , 0.001 , $x_g = -10$, -20 , -50 and $y_g = 0$. The speed and power of the resulting gaits are plotted in Figure. 3 as red stars. The gaits with $\alpha = 1$, $\beta = 0.01$, and $x_g = -20$ are circled in black, to illustrate the performance of a unique set of parameters accross all three environments.

These results confirm that MPC can synthesize effective locomotion gaits in all tested conditions. Furthermore, the resulting gaits are comparable to, and occasionally better than their most efficient serpenoid curve counterparts. For example, in the environment dominated by the dry friction, 3 sets of the MPC implementation generate gaits with speed around 1.6 m/s and power around 35 W. The Pareto-optimal gaits with the similar level of power can only achieve the speed around 1.1 m/s. In the viscous fricton dominated environment and the fluid dynamics, all MPC-generated gaits are around the Pareto optimal trade-offs between the power consumption and the speed.

Beyond efficiency, we believe that one of the most attractive characteristics of automated gait synthesis is its generalizability accross different environments. We note that a single set of parameters ($\alpha = 1$, $\beta = 0.01$, and $x_g = -20$, circled in black in the figure) produces effective gaits for all environments. In contrast, comparable behavior can be obtained with serpenoid curves only with environment-specific parameter tuning.

To obtain further insight, we studied the gait produced by MPC with parameters $\alpha = 1$, $\beta = 0.01$ using a Discrete Fourier Transform (DFT). For each environment, we computed the major frequency component, the amplitude, and phase offset for each joint in the respective gait. The results are listed in Table III. We note that the resulting gaits are qualitatively different. For the gait produced using fluid dynamic effects, the joints at the tail of the snake move at a significantly higher amplitude that the ones at the head, much more so than in the other two environments. This qualitatively mirrors behaviors observed in nature for similar enviroments, as in the case of eel-like anguilliform gaits [29] and fish-like carangiform gaits [30].

C. Automatic Generation of Complex Gaits

The gaits we have shown so far to illustrate our method, while efficient and generalizable accross different environ-

TABLE III
DFT OF MPC GAITS IN DIFFERENT ENVIRONMENTS

Environment	Frequency(Hz)				Amplitude(rad)			
	f_1	f_2	f_3	f_4	α_1	α_2	α_3	α_4
Dry	6.31	6.31	6.31	6.31	0.25	0.32	0.37	0.42
Viscous	6.75	6.75	6.75	6.75	0.53	0.62	0.67	0.83
Fluid	5.25	5.25	5.25	5.25	0.51	0.76	1.40	2.42

ments, are still serpenoid-like in nature. However, the proposed method for gait synthesis can also generate more complex gaits, without having to adhere to the serpenoid template. This can be achieved with the use of different cost functions or goal settings.

Fig. 4 illustrates this concept. The top image shows a gait generated by using the same cost function used so far, but with a goal position for the snake head that induces a sharp turn (as opposed to a goal set in front of the snake, as before). The result is an effective turning motion that does not rely on a single-frequency serpenoid pattern. The bottom image illustrates the use of the obstacle-based component of the cost function shown in Eq. (18). Here, the gait is still serpenoid in nature, but the amplitudes of the different joints are automatically adjusted as the snake moves through the tunnel. At any point, the links outside the narrowest point of the tunnel are used to propel forward, while the links in the tunnel are kept still to avoid collision. Both gaits are also shown in the video accompanying the submission, as are additional results illustrative of our method.

D. Practical Applicability

The proposed MPC-based gait generation method faces two important challenges for application to real robots: the reliance on dynamic models, and the computational effort. For real-life execution, the dynamic model will only be an approximation of real-life physics. Furthermore, gait generation must keep up with execution in order to be used online for a real robot.

To study computational performance, we measured the time needed to optimize a single trajectory with a horizon of 25 steps. We use a control rate of 100 Hz, meaning that such a 25-step trajectory comprises 0.25 s of real life execution. We averaged computational performance over a complete 6 s locomotion gait for each environment. For dry friction, viscous friction and fluid dynamics, average computation times where 1.4 s, 1.0 s, and 1.0 s respectively. Standard deviations where 1.4 s, 0.6 s, and 0.5 s respectively. All tests where performed on a commodity 16-core AMD Ryzen 7 PRO 1700 processor.

We notice that, in our current implementation, the iLQR algorithm is not efficient enough for real-life execution. For example, in the case of viscous friction, it takes 1 s of computation time to optimize a trajectory that takes 0.25 s to execute. We estimate that, for practical applicability, a computation speed-up of at least 10X to 20X will be necessary; this could be achieved via an optimized implementation, more extensive parallelization, or algorithmic improvements. We will pursue all these directions in future work.

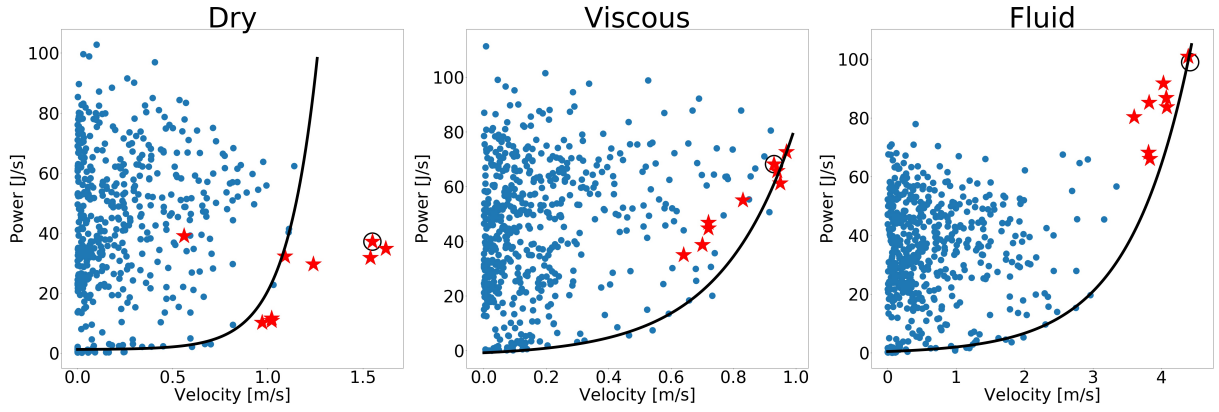


Fig. 3. Distribution of power consumption with the forward speed and Pareto-optimal front for the serpenoid curve gaits. The blue points are the result of the serpenoid curve grid search, and the black line is the respective Pareto front. The red stars are gaits generated by MPC. The stars circled in black are generated with the gait from $\alpha = 1.0$, $\beta = 0.1$, and $x_g = -10$

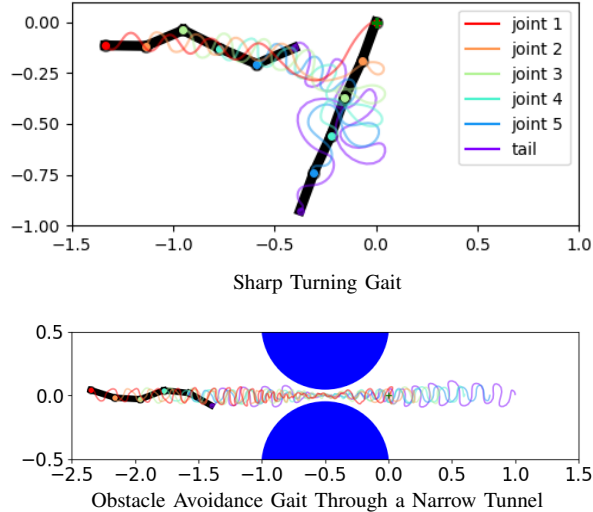


Fig. 4. MPC generates flexible gaits adaptive to environments. The top figure demonstrates a sharp turning gait. The bottom figure demonstrates obstacle avoidance through a narrow tunnel.

To study robustness to errors in the dynamics model, we performed a preliminary test of how performance using viscous friction is affected by errors in the friction coefficient. We thus introduced a discrepancy between the friction coefficient used by MPC to generate the gait, and the one used to test it. For a 5% error in the transverse friction coefficient, we observed a 2% reduction in the trajectory speed; a 25% error produced a 4% slowdown. However, the dynamics model contains numerous parameters, which can all affect performance; a more complete evaluation of these effects will be needed for real-life applications.

VII. CONCLUSIONS AND FUTURE WORK

In this paper, we proposed a method for automatic gait synthesis for snake robots using iLQR, a trajectory optimization method from the MPC family. Unlike methods that use a serpenoid curve or similar patterns, this approach produces gaits without relying on predefined patterns, by optimizing the trajectory w.r.t. a given cost function. The key is the use of a model of the dynamics of the system, for which we use a

standard time-stepping scheme with explicit integration and Newton-Euler chain dynamics at each time step.

To encapsulate the characteristics of each environment, we used models of the anisotropic reaction forces that arise in response to snake movements. For the case of dry friction, we introduced a novel model that approximates anisotropic Coulomb friction with a smooth friction force vs. velocity profile, by integrating the Maximum Dissipation Principle. Other reaction forces models we used include viscous friction as well as fluid dynamic effects such as drag and added mass. Together, these reaction forces allow us to model three different environments for undulatory locomotion: overland on solid media, underwater in a low Reynolds number regime (small scale swimmers), and underwater in a large Reynolds number regime (large swimmers). It is, to the best of our knowledge, the first time that an automatic gait generation approach has been used to generate and analyze undulatory gaits across different environment models.

Our key result shows that, without any tuning or change in parameters between environments, the proposed automatic gait synthesis method produces gaits that are as efficient as those obtained by manually tuning a serpenoid curve to each environment. The undulatory gaits produced by the proposed method also display some of the characteristics observed in nature. However, as it does not depend on a pre-defined movement pattern, the same method can produce more complex gaits, e.g. for sharp turns or obstacle avoidance, by using different formulations for the optimized cost function.

Before these results can be used for gait generation on real robots, additional challenges still have to be tackled. In particular, a reduction in computation time is needed to meet the requirements of keeping up with real-life execution. Nevertheless, we believe that automatic gait generation methods as the one presented here can represent a useful complement to approaches based on a central pattern generator, as we aim towards robot snakes able to operate in complex, unstructured environments.

REFERENCES

- [1] S. Hirose, "Biologically inspired robots: Snake-like locomotors and manipulators," *Robotica*, vol. 12, p. 282282, 1994.
- [2] K. Y. Pettersen, "Snake robots," *Annual Reviews in Control*, vol. 44, pp. 19 – 44, 2017. [Online]. Available: <http://www.sciencedirect.com/science/article/pii/S1367578817301050>
- [3] C. Gong, M. J. Travers, H. C. Astley, L. Li, J. R. Mendelson, D. I. Goldman, and H. Choset, "Kinematic gait synthesis for snake robots," *The International Journal of Robotics Research*, vol. 35, no. 1-3, pp. 100–113, 2016. [Online]. Available: <https://doi.org/10.1177/0278364915593793>
- [4] S. Ma, "Analysis of snake movement forms for realization of snake-like robots," vol. 4, pp. 3007–3013 vol.4, May 1999.
- [5] A. J. Ijspeert, "Central pattern generators for locomotion control in animals and robots: A review," *Neural Networks*, vol. 21, no. 4, pp. 642 – 653, 2008, robotics and Neuroscience. [Online]. Available: <http://www.sciencedirect.com/science/article/pii/S0893608008000804>
- [6] P. Prautsch and T. Mita, "Control and analysis of the gait of snake robots," in *Proceedings of the 1999 IEEE International Conference on Control Applications (Cat. No.99CH36328)*, vol. 1, Aug 1999, pp. 502–507 vol. 1.
- [7] J. Whitman, F. Ruscelli, M. Travers, and H. Choset, "Shape-based compliant control with variable coordination centralization on a snake robot," in *2016 IEEE 55th Conference on Decision and Control (CDC)*, Dec 2016, pp. 5165–5170.
- [8] F. Sanfilippo, J. Azpiazu, G. Marafioti, A. Transeth, O. Stavdahl, and P. Liljeback, "Perception-driven obstacle-aided locomotion for snake robots: The state of the art, challenges and possibilities," *Applied Sciences*, vol. 7, p. 336, 03 2017.
- [9] M. Saito, M. Fukaya, and T. Iwasaki, "Serpentine locomotion with robotic snakes," *IEEE Control Systems Magazine*, vol. 22, no. 1, pp. 64–81, Feb 2002.
- [10] E. Kelasidi, M. Jesmani, K. Y. Pettersen, and J. T. Gravdahl, "Locomotion efficiency optimization of biologically inspired snake robots," 2018.
- [11] D. Rollinson, K. V. Alwala, N. Zevallos, and H. Choset, "Torque control strategies for snake robots," in *2014 IEEE/RSJ International Conference on Intelligent Robots and Systems*, Sep. 2014, pp. 1093–1099.
- [12] J. Mukherjee, S. Mukherjee, and I. N. Kar, "Sliding mode control of planar snake robot with uncertainty using virtual holonomic constraints," *IEEE Robotics and Automation Letters*, vol. 2, no. 2, pp. 1077–1084, April 2017.
- [13] K. Kon, M. Tanaka, and K. Tanaka, "Mixed integer programming-based semiautonomous step climbing of a snake robot considering sensing strategy," *IEEE Transactions on Control Systems Technology*, vol. 24, no. 1, pp. 252–264, Jan 2016.
- [14] M. Tesch, J. Schneider, and H. Choset, "Using response surfaces and expected improvement to optimize snake robot gait parameters," in *2011 IEEE/RSJ International Conference on Intelligent Robots and Systems*. IEEE, 2011, pp. 1069–1074.
- [15] E. Kelasidi, M. Jesmani, K. Pettersen, and J. Gravdahl, "Locomotion efficiency optimization of biologically inspired snake robots," *Applied Sciences*, vol. 8, no. 1, p. 80, 2018.
- [16] Z. Bing, C. Lemke, Z. Jiang, K. Huang, and A. Knoll, "Energy-efficient slithering gait exploration for a snake-like robot based on reinforcement learning," *CoRR*, vol. abs/1904.07788, 2019. [Online]. Available: <http://arxiv.org/abs/1904.07788>
- [17] G. Sartoretti, W. Paivine, Y. Shi, Y. Wu, and H. Choset, "Distributed learning of decentralized control policies for articulated mobile robots," *CoRR*, vol. abs/1901.08537, 2019. [Online]. Available: <http://arxiv.org/abs/1901.08537>
- [18] Y. Tassa, T. Erez, and E. Todorov, "Synthesis and stabilization of complex behaviors through online trajectory optimization," in *2012 IEEE/RSJ International Conference on Intelligent Robots and Systems*. IEEE, 2012, pp. 4906–4913.
- [19] J. Ostrowski and J. Burdick, "The geometric mechanics of undulatory robotic locomotion," *The international journal of robotics research*, vol. 17, no. 7, pp. 683–701, 1998.
- [20] V. Mehta, S. Brennan, and F. Gandhi, "Experimentally verified optimal serpentine gait and hyperredundancy of a rigid-link snake robot," *IEEE Transactions on Robotics*, vol. 24, no. 2, pp. 348–360, April 2008.
- [21] D. E. Stewart, "Rigid-body dynamics with friction and impact," *SIAM review*, vol. 42, no. 1, pp. 3–39, 2000.
- [22] R. L. Hatton and H. Choset, "Geometric swimming at low and high reynolds numbers," *IEEE Transactions on Robotics*, vol. 29, no. 3, pp. 615–624, June 2013.
- [23] E. Kelasidi, K. Y. Pettersen, J. T. Gravdahl, and P. Liljeback, "Modeling of underwater snake robots," in *2014 IEEE International Conference on Robotics and Automation (ICRA)*, May 2014, pp. 4540–4547.
- [24] W. Khalil, G. Gallot, and F. Boyer, "Dynamic modeling and simulation of a 3-d serial eel-like robot," *IEEE Transactions on Systems, Man, and Cybernetics, Part C (Applications and Reviews)*, vol. 37, no. 6, pp. 1259–1268, Nov 2007.
- [25] A. Filippov, G. Westhoff, A. Kovalev, and S. Gorb, "Numerical model of the slithering snake locomotion based on the friction anisotropy of the ventral skin," *Tribology Letters*, vol. 66, no. 3, p. 119, 2018.
- [26] D. E. Stewart and J. C. Trinkle, "An implicit time-stepping scheme for rigid body dynamics with inelastic collisions and coulomb friction," *International Journal for Numerical Methods in Engineering*, vol. 39, no. 15, pp. 2673–2691, 1996.
- [27] P. Liljeback, K. Y. Pettersen, Ø. Stavdahl, and J. T. Gravdahl, *Snake robots: modelling, mechatronics, and control*. Springer Science & Business Media, 2012.
- [28] A. D. Belegundu and T. R. Chandrupatla, *Optimization concepts and applications in engineering*. Cambridge University Press, 2019.
- [29] K. A. McIsaac and J. P. Ostrowski, "Motion planning for anguilliform locomotion," *IEEE Transactions on Robotics and Automation*, vol. 19, no. 4, pp. 637–652, Aug 2003.
- [30] K. A. Morgansen, V. Duidam, R. J. Mason, J. W. Burdick, and R. M. Murray, "Nonlinear control methods for planar carangiform robot fish locomotion," in *Proceedings 2001 ICRA. IEEE International Conference on Robotics and Automation (Cat. No.01CH37164)*, vol. 1, May 2001, pp. 427–434 vol.1.